

# Ground-State Clusters for Short-Range Attractive and Long-Range Repulsive Potentials

S. Mossa,<sup>\*,†,‡</sup> F. Sciortino,<sup>\*,†</sup> P. Tartaglia,<sup>§</sup> and E. Zaccarelli<sup>†</sup>

*Dipartimento di Fisica and INFM Udr and SOFT: Complex Dynamics in Structured Systems, Università di Roma "La Sapienza", P.le A. Moro 2, I-00185, Roma, Italy, European Synchrotron Radiation Facility, B.P. 220, F-38043 Grenoble, Cedex France, and Dipartimento di Fisica and INFM Udr and SMC: Center for Statistical Mechanics and Complexity, Università di Roma "La Sapienza", P.le A. Moro 2, I-00185, Roma, Italy*

Received June 11, 2004. In Final Form: September 9, 2004

We report calculations of the ground-state energies and geometries for clusters of different sizes (up to 80 particles), where individual particles interact simultaneously via a short-ranged attractive potential, modeled with a generalization of the Lennard-Jones potential, and a long-ranged repulsive Yukawa potential. We show that for specific choices of the parameters of the repulsive potential, the ground-state energy per particle has a minimum at a finite cluster size. For these values of the parameters in the thermodynamic limit, at low temperatures and small packing fractions, where clustering is favored and cluster–cluster interactions can be neglected, thermodynamically stable cluster phases can be formed. The analysis of the ground-state geometries shows that the spherical shape is marginally stable. In the majority of the studied cases, we find that above a certain size, ground-state clusters preferentially grow almost in one dimension.

## I. Introduction

Understanding the formation of self-assembled structures at the nano- and mesoscopic levels is one of the central issues in condensed matter studies,<sup>1</sup> particularly in biological and soft matter fields. More recently, significant efforts have been made in the direction of finding connections between features of the interparticle potential and the resulting stable supraparticle patterns. In this respect, an interesting class of systems in which particles self-assemble into large aggregates is generated by systems of particles interacting simultaneously via an attractive potential (which can be of van der Waals or depletion origin) and a repulsive interaction (usually of screened electrostatic origin). In density and temperature conditions where the attractive part of the potential would generate macroscopic phase separations, the presence of a repulsive part contrasts the phase separation process, leaving the system, in some cases, in a microphase separated condition. The competition between attraction and repulsion generates the formation of equilibrium phases where stable clusters of particles are formed (sometimes called cluster or micellar phases) or even of more complex structures (such as lamellar or columnar phases). Experimental evidence for such thermodynamically stable cluster phases has been recently presented for colloidal systems and for solutions of proteins at low ionic strength.<sup>2–6</sup> Cluster phases have also been observed in aqueous solutions of silver iodide.<sup>7</sup> Theoretically, the

formation of phases with different morphology has been addressed within lattice models and mean field calculations for unscreened electrostatic interactions<sup>8–13</sup> and, more recently, in colloidal science, explicitly accounting for ion condensation around particles.<sup>14</sup> Numerical evidence of cluster phases has also been recently reported.<sup>12,15–17</sup> Interestingly, at low densities, particles aggregates can act as monomers of a supramolecular liquid, showing phenomena typical of the liquid state such as crystallization and glass transition.<sup>15</sup>

In this work, we study an off-lattice three-dimensional representative model of particles interacting via a short-range attraction (which we model with the generalization to very large  $\alpha$  of the Lennard-Jones (LJ)  $2\alpha - \alpha$  potential, as previously proposed by Vliegthart et al.<sup>18</sup>) complemented by a long-range repulsion, which we model by a screened electrostatic Yukawa potential. Screening is included in the model, since we are mostly interested in describing charged colloidal and protein solutions, where addition of salt in the dispersant medium provides an

\* To whom correspondence should be addressed. E-mail: mossa@esrf.fr; francesco.sciortino@phys.uniroma1.it.

† Dipartimento di Fisica and INFM Udr and SOFT: Complex Dynamics in Structured Systems, Università di Roma "La Sapienza".

‡ European Synchrotron Radiation Facility.

§ Dipartimento di Fisica and INFM Udr and SMC: Center for Statistical Mechanics and Complexity, Università di Roma "La Sapienza".

(1) See, for example: Safran, S. A. *Statistical Thermodynamics of Surfaces, Interfaces, & Membranes*; Westview Press: Boulder, CO, 2003. Lindoy, L. F.; Atkinson, I. M. *Self-Assembly in Supramolecular Systems*; Royal Society of Chemistry: Cambridge, 2001.

(2) Baglioni, P.; Fratini, E.; Lonetti, B.; Chen, S. H. *J. Phys.: Condens. Matter* **2004**, *16*, S5003.

(3) Stradner, A.; Sedgwick, H.; Cardinaux, F.; Poon, W. C. K.; Egelhaaf, S. U.; Schurtenberger, P. *Nature (London)*, in press.

(4) Segre, P. N., et al. *Phys. Rev. Lett.* **2001**, *86*, 6042.

(5) Dinsmore, A. D.; Weitz, D. A. *J. Phys.: Condens. Matter* **2002**, *14*, 7581.

(6) Sedgwick, H., et al. Preprint cond-mat/0309616.

(7) Mladenovic, I.; Kegel, W. K.; Bomas, P.; Freederik, P. M. *J. Phys. Chem. B* **2003**, *107*, 5717.

(8) Grousson, M.; Tarjus, G.; Viot, P. *Phys. Rev. E* **2000**, *62*, 7781.

(9) Löw, U.; Emery, V. J.; Fabricius, K.; Kivelson, S. A. *Phys. Rev. Lett.* **1994**, *72*, 1918.

(10) Schmaliam, J.; Wolynes, P. G. *Phys. Rev. Lett.* **2000**, *85*, 836.

(11) Wu, D.; Chandler, D.; Smit, B. *J. Phys. Chem.* **1992**, *96*, 4077.

(12) Sear, R. P.; Vhung, S.-W.; Markovick, G.; Gelbart, W. M.; Heath, J. R. *Phys. Rev. E* **1999**, *59*, R6255.

(13) Lorenzana, J.; Castellani, C.; Di Castro, C. *Phys. Rev. B* **2001**, *64*, 235127.

(14) Groenewold, J.; Kegel, W. K. *J. Phys. Chem. B* **2001**, *105*, 11702.

(15) Sciortino, F.; Mossa, S.; Zaccarelli, E.; Tartaglia, P. *Phys. Rev. Lett.* **2004**, *93*, 055701.

(16) Sator, N.; Fierro, A.; Del Gado, E.; Coniglio, A. Preprint cond-mat/0312591.

(17) Imperio, A.; Reatto, L. *J. Phys.: Condens. Matter* **2004**, *16*, S3769.

(18) Vliegthart, G. A.; Lodge, J. F. M.; Lekkerkerker, H. N. W. *Physica A* **1999**, *263*, 378.

efficient mechanism of reduction of the repulsive interaction range. Modeling the short-range attraction with the Lennard-Jones  $2\alpha - \alpha$  potential is of course arbitrary, but at the same time representative (by tuning the exponent  $\alpha$ ) of all short-range potentials, arising either from depletion interactions or from van der Waals forces. For different choices of the repulsive potential parameters, we calculate the ground-state energy and structure of clusters of different size, to evaluate the conditions under which stable cluster phases are expected at low temperatures, where entropic effects can be neglected. We show that on varying the range of interaction and the intensity of the long-range repulsive potential, it is possible to obtain stable cluster structures of different geometries. To locate the ground-state structures and their energies, we have used a modified version of the basin-hopping algorithm<sup>19</sup> which has been proposed and extensively applied in models of simple liquids and molecular systems. To extend the range of studied cluster sizes beyond what is possible with present numerical resources, we complement the ground-state calculations by analytic calculations of the cluster self-energy, under the assumption of spheric cluster shape.

The paper is organized as follows. Section II contains a study of the cluster ground states for the  $2\alpha - \alpha$  attractive potential for two values of  $\alpha$ , typical of short-range attractive interactions. A comparison of ground-state energies and cluster shapes between the short-range attractive potential and both the standard  $\alpha = 6$  case (from ref 19) and the hard sphere (HS) case (from ref 20) is also reported. In section III, we present cluster energies and geometries resulting from the addition of a repulsive Yukawa potential, for different values of the potential parameters. Section IV is devoted to the analytic calculation of the cluster self-energy under the assumption of spherical shape. Finally, section V contains a discussion of the results and conclusions.

## II. Cluster Ground States for the Attractive Short-Range $2\alpha - \alpha$ Potential

Short-range attractive interactions arise in colloidal systems either from van der Waals interactions (integrated over the volume of the interacting particles) or via a depletion mechanism, that is, when particles of intermediate dimension between the suspended colloids and the solvent molecules are added to the solution.<sup>21</sup> Here we model the short-range attractive potential in a numerically convenient way with the generalization of the Lennard-Jones potential, namely, the  $2\alpha - \alpha$  potential, previously proposed by Vliegthart et al.,<sup>18</sup>

$$V_{2\alpha-\alpha}(r) = 4\epsilon \left[ \left( \frac{\sigma}{r} \right)^{2\alpha} - \left( \frac{\sigma}{r} \right)^\alpha \right] \quad (1)$$

where the value of  $\alpha$ , which in the standard LJ case is fixed to 6, is varied to control the range of interactions. In what follows, we have chosen  $\epsilon$  and  $\sigma$  as the units of energy and length, respectively. We focus our attention on three values of the parameter  $\alpha$  that are relevant for our discussion. First,  $\alpha = 100$ , which corresponds to an attractive range of the order of a few percent of  $\sigma$ , typical of very narrow-ranged depletion interactions. Next, we consider the case  $\alpha = 18$ , which corresponds to the case for which the value of the potential energy at the distance of the second neighbor shell becomes negligible. Finally,

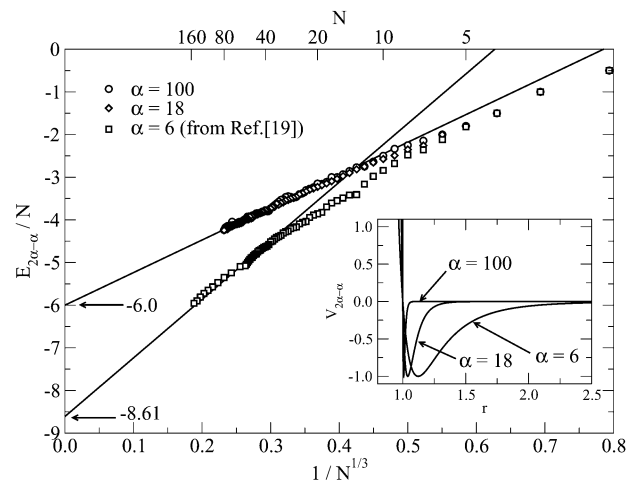


**Figure 1.** Ground-state energy per particle as a function of  $1/N^{1/3}$  ( $N$  on the top x-axis) for the  $2\alpha - \alpha$  potential at the indicated values of  $\alpha$ . The values of the energy per particle for the fcc crystal structure are indicated by arrows. Inset: Radial dependence of interaction potential  $V_{2\alpha-\alpha}$  for the three studied values of  $\alpha$ .

for comparison, we also report results from ref 19, for the Lennard-Jones case  $\alpha = 6$ . The three potentials ( $\alpha = 100$ , 18, and 6) are illustrated in the inset of Figure 1.

The problem of locating the most stable state (ground state) on a complicated potential energy surface (PES) is a hard one. Indeed, theoretical general arguments ensure that there is no algorithm that is certain to solve such a problem within a reasonable time scale. Moreover, in the case one should be able to find the ground state, there exists no way to prove that it is unique. Therefore, the best one can do is to find a bona fide, putative ground state.

Among many other techniques, that is, genetic algorithms or hypersurface deformation methods, the basin-hopping global optimization technique,<sup>19</sup> introduced by Wales and Doye, has been found to be particularly efficient in localizing the putative ground state for clusters (both atomic and molecular) of up to a few hundred particles, interacting by means of several interaction potentials. Such an algorithm consists of a constant-temperature Monte Carlo simulation where the actual potential energy surface is transformed into a stairlike surface by replacing the potential energy function with the values of the potential energy of the closest local minimum, named the inherent structure.<sup>22</sup> The acceptance criterion is thus based upon the change in the inherent structure energy.

The efficiency of this method lies in the fact that it removes the transitional state regions. This procedure does not affect the energy of the minima but allows the system to explore the relevant minima on the original PES in a much faster way. Indeed, on the original PES, among all trajectories approaching the boundaries between two basins of attraction, only the one following a transition state is likely to hop from one minimum to the other. At variance, on the transformed PES the system is allowed to hop at any point along the basin boundary. This very fact reduces dramatically the time scale for interbasin motion and therefore for relaxation to the lowest energy state.

We also note that the qualitative and quantitative conclusions of this study do not depend on identification of the absolute ground-state configuration in the large- $N$  limit.

(19) Wales, D. J.; Doye, J. P. K. *J. Phys. Chem. A* **1997**, *101*, 5111.

(20) Sloane, N. J. A.; Hardin, R. H.; Duff, T. S.; Conway, J. H. *Disc. Comp. Geom.* **1995**, *14*, 237.

(21) Israelachvili, J. N. *Intermolecular and Surface Forces*, 2nd ed.; Academic Press: London, 1992.

(22) Stillinger, F. H.; Weber, T. A. *Phys. Rev. A* **1982**, *25*, 978; *Science* **1984**, *225*, 983. Stillinger, F. H. *Science* **1995**, *267*, 1935.

Here, to calculate the ground-state energy of clusters of different size  $N$  and their geometry, we have used a modified version of the basin-hopping algorithm.<sup>19</sup> To further favor barrier crossing, every 100 Monte Carlo steps, the less bounded atom is removed and reinserted in the position with the lowest insertion energy. The largest cluster size studied is of the order of 80 particles.

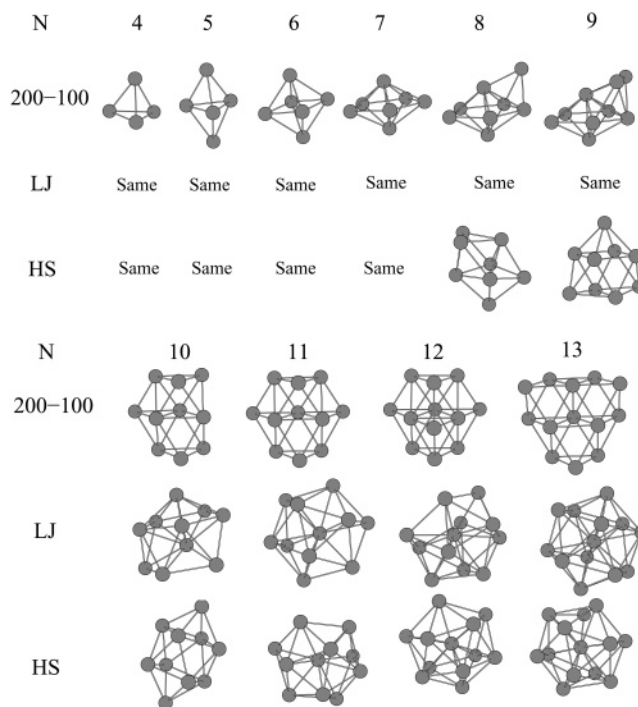
Figure 1 shows the ground-state energy per particle  $E/N$  as a function of  $N^{-1/3}$ , for all three values of  $\alpha$ . Data are reported as a function of  $N^{-1/3}$  since, for large clusters, one expects to observe the functional form  $E/N = c_0 + c_1/N^{1/3}$ . Indeed, the cluster energy can be expressed as the sum of a bulk term,  $c_0N$ , and a surface term,  $c_1N^{2/3}$ . We find that for  $\alpha = 100$ , when clusters are larger than  $\approx 13$ –15 particles, the ground-state energy per particle is well represented by the fit  $E/N = -5.937 + 7.435/N^{1/3}$ , providing an estimate for the bulk energy compatible with a close-packed face-centered cubic (fcc) or hexagonal close-packed (hcp) crystalline ordering value ( $-6$ ). The  $\alpha = 18$  data are practically indistinguishable from the  $\alpha = 100$  case, suggesting that cluster ground-state energies and geometries are the same for all potentials with  $\alpha \geq 18$ .

Figure 1 also reports the ground-state energy per particle for the standard Lennard-Jones case  $\alpha = 6$ , from ref 19. As compared to the shorter range case, the ground-state energy of the LJ is lower, due to the attractive contributions arising from second and further neighbors. The asymptotic behavior (with  $N^{-1/3}$ ) is approached at much larger sizes (order of  $\approx 30$ –40 particles) and suggests an extrapolation to the bulk value, consistent with the estimate for the LJ fcc or hcp values of  $-8.61$ .<sup>23</sup>

The sign of the surface term, that is, the sign of  $c_1$ , provides information on the thermodynamic behavior of a macroscopic system at low temperatures. Indeed, when  $T$  is low, the ground-state energy becomes the relevant thermodynamic potential. The condition  $c_1 > 0$  ensures that the system ground state in the thermodynamic limit is composed by a single macroscopic bulk cluster. In the cluster-based thermodynamic description pioneered by Hill,<sup>24</sup>  $c_1 > 0$  indicates that at low temperatures the system will phase separate in a dense bulk liquid in equilibrium with a gas phase.

Next, we discuss the geometry of the ground-state clusters. Figure 2 contrasts the cluster geometries for the short-range case with the LJ case. For very small  $N$ , the structure of the clusters is independent of the range of the potential. For  $N < 10$ , the structure of the clusters does not change with  $\alpha$ . For larger  $N$  values, the geometry changes significantly, since the constraint induced by the short range of the potential ( $\alpha \geq 18$ ) facilitates a progressive layering. For example, for the case  $N = 13$ , the icosahedron structure, which is particularly stable in the LJ case,<sup>19</sup> is not observed in the short-range case.

It is instructive to compare these results also with hard sphere cluster geometries, calculated theoretically minimizing the second moment of the mass distribution  $M^{20,25}$  and recently measured with a new experimental technique introduced to produce compact clusters of controlled numbers of small colloidal particles.<sup>26</sup> For  $N < 11$ , these clusters have been found to be identical to those calculated



**Figure 2.** Cluster structures for  $4 \leq N \leq 13$  for the  $\alpha = 100$ , 18 potential, Lennard Jones (ref 19), and hard spheres (ref 20). “Same” indicates when the structure is identical to the  $\alpha = 100$ , 18 case.

in ref 20. The third row of Figure 2 reports the HS clusters from ref 20. As for the comparison with the LJ case, for  $N \leq 7$  all clusters have the same structure, while for  $N > 7$  differences in the potential start to be significant.

### III. The Competition between Attraction and Repulsion Terms

In this section, we report calculations of the cluster ground-state energy for a potential composed by a short-range attractive part (modeled only with  $\alpha = 100$ , since we have shown previously that  $\alpha = 18$  cannot be distinguished from the  $\alpha = 100$  case) complemented by a screened electrostatic repulsive interaction modeled by a Yukawa potential,

$$V_Y(r) = A \frac{e^{-r/\xi}}{r/\xi} \quad (2)$$

The resulting total potential is thus  $V(r) = V_{2\alpha-\alpha} + V_Y$ . In the following,  $A$  is given in units of  $\epsilon$  and  $\xi$  in units of  $\sigma$ . Figure 3 shows the shape of the total potential for different  $\xi$  and  $A$  values. The resulting potential is conceptually similar to the well-known Derjaguin–Landau–Verwey–Overbeek (DLVO) potential,<sup>27</sup> even if it differs for the absence of the weak secondary minima and the finite value of the attractive interaction energy.

Figure 4 shows the ground-state energy per particle  $E/N$  for different  $A$  and  $\xi$  values. The same minimization procedure as described in the previous section has been implemented, with the additional condition that, in the search procedure, moves creating disconnected clusters are rejected. For appropriate values of  $A$  and  $\xi$  (for example  $A = 0.2$  and  $\xi = 2.0$ ), the cluster ground-state energy shows a minimum at a finite size  $N^*$ , indicating that clusters of size larger than  $N^*$  are energetically disfavored. A simple

(23) Stillinger, F. H. *J. Chem. Phys.* **2001**, *115*, 5208.

(24) Hill, T. L. *An Introduction to Statistical Thermodynamics*; Dover: New York, 1987.

(25) The physical processes underlying the observations of ref 26 have been studied in: Lauga, E.; Brenner, M. P. Preprint cond-mat/0404236. Here the authors clarify the reasons for which the final packings are unique and why they minimize a purely geometrical quantity like the second moment.

(26) Manoharan, V. N.; Elsesser, M. T.; Pine, D. J. *Science* **2003**, *301*, 483.

(27) Derjaguin, B. V.; Landau, L. V. *Acta Physicochim. USSR* **1941**, *14*, 633. Verwey, E. J. W.; Overbeek, J. T. *Theory of Stability of Lyophobic Colloids*; Elsevier: Amsterdam, 1948.

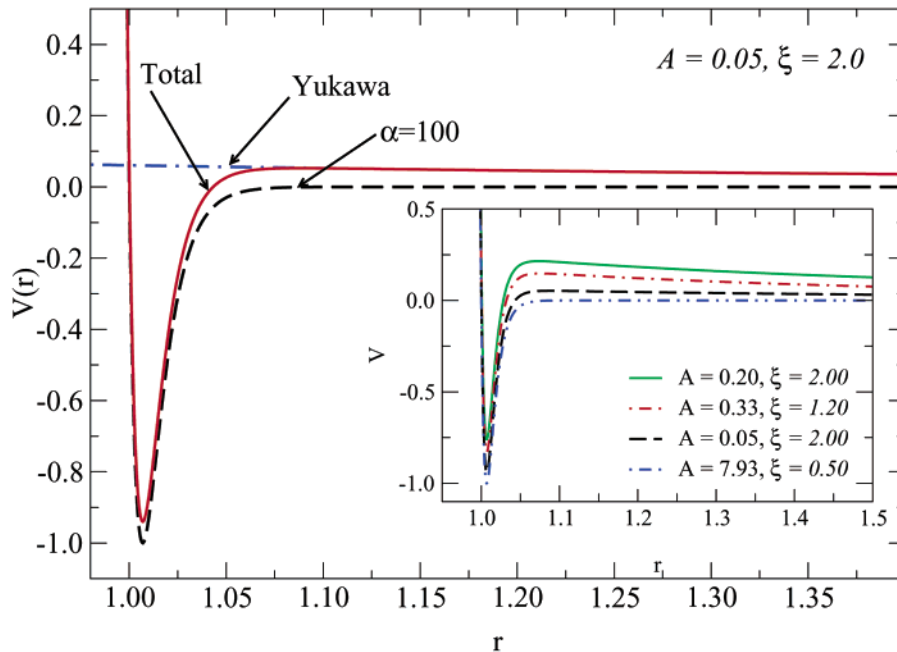


**Figure 3.** Short-range attractive  $2\alpha - \alpha$  potential (dashed line), long-range Yukawa repulsive potential (dotted-dashed line), and total potential (solid line) for  $A = 0.05$  and  $\xi = 2.0$ . Inset:  $V_{2\alpha-\alpha} + V_Y$  at the indicated values of  $A$  and  $\xi$ .

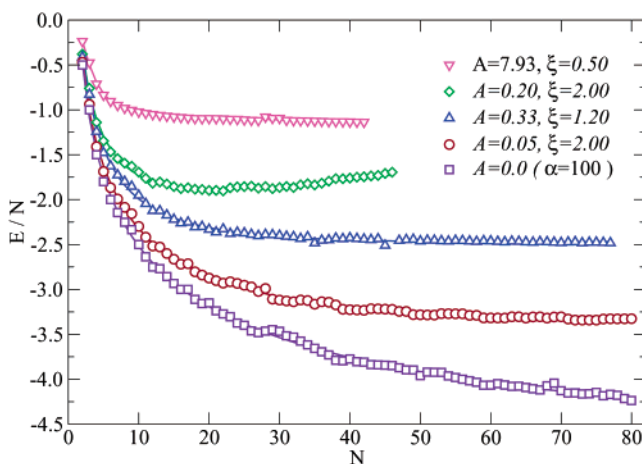


**Figure 4.** Ground-state energies per particle for five different choices of the potential parameters. The energies have been calculated by basin-hopping Monte Carlo optimization (ref 19), as discussed in the text.

physical explanation of the existence of an optimal size can be given as follows. At large enough  $N$ , the addition of an extra layer of particles will contribute to the energy with a negative term due to the attractive nearest neighbor interactions (which involves only interactions with particles in the surface layer due to the short range of the potential) plus a positive contribution arising from the Yukawa repulsion which, due to its longer range, involves instead a large fraction of particles in the cluster. The balance between these two terms provides a condition for  $N^*$ . Of course, the larger the amplitude or the longer the range of the repulsion, the smaller the  $N^*$ . The fact that an optimal finite cluster size is observed suggests that a macroscopic system at low temperature will not form a single aggregate but will prefer to partition the particles into clusters of size  $N^*$ . In this respect, liquid condensation is inhibited and the structure of the system at low temperature and low packing fractions will be constituted by a cluster phase. At finite temperatures, entropic

contributions to the free energy will become important and will always favor the stability of clusters of size smaller than  $N^*$ . Hence,  $N^*$  plays the role of an upper limit for the cluster size.<sup>28</sup> In other cases, a minimum is not found, but the energy per particle becomes essentially flat. In these conditions, the ground state of a macroscopic system will be composed by a highly polydisperse cluster phase.

In Figure 5, we compare the ground-state cluster geometries for  $N = 38$  calculated for different choices of the Yukawa parameters. At fixed cluster size, by changing the potential parameters the cluster structure can be tuned from almost spherical to almost one-dimensional. A similar crossover has been found in Dzugutov potentials.<sup>29</sup> The studied parameters encompass situations occurring in uncharged colloids ( $A = 0$ ) and those typical of charged colloids ( $A > 0$ ) in apolar solvents or weakly screened polar solvents. Indeed,  $A$  is proportional to the effective charge of the colloidal particle, while the screening length  $\xi$  is controlled by the ionic strength. In the absence of salt,  $\xi$  depends only on colloid concentration, and a small screening is produced by the counterions in the solvent.<sup>27,30,31</sup>

Figure 6 shows the  $N$ -dependence of the cluster geometry, for the case  $A = 0.05$  and  $\xi = 2$ , to highlight the changes in the preferential geometry with cluster size. It appears that the geometry of the clusters is strongly size dependent. To convey this point, we show in Figure 7 the

(28) The results reported in Figure 4 are thermodynamic results and do not imply a specific growth mechanism. In general, clusters can grow both by cluster-cluster aggregation or by cluster-monomer aggregation. Also, the lifetime of each cluster, between distinct coalescence and growth events, may not be sufficient for the establishment of a thermodynamic equilibrium configuration. In this respect, the size dependence of the ground-state energy does not describe the process of cluster growth. Still, the calculated size dependence of the ground-state energy allows us to estimate if, under specific choices of the parameters, aggregation will proceed indefinitely or if the driving force for aggregation will vanish beyond a critical size, in which case, even in a diffusion-controlled growth regime, aggregation will stop.

(29) Doye, J. P. K.; Wales, D. J.; Simdyankin, S. I. *Faraday Discuss.* **2001**, *118*, 159. Doye, J. P. K.; Wales, D. J.; Zetterling, F. H. M.; Dzugutov, M. *J. Chem. Phys.* **2003**, *118*, 2792.

(30) Likos, C. N. *Phys. Rep.* **2002**, *348*, 267.

(31) Denton, A. R. *J. Phys.: Condens. Matter* **1999**, *11*, 10061.

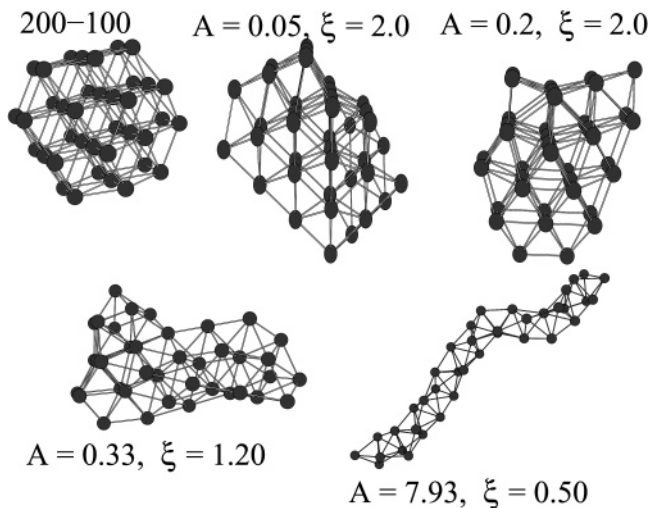


**Figure 5.** Ground-state clusters for  $N = 38$  for the indicated potentials. On changing the values of the parameters, it is possible to interpolate from a close-packed to an almost unidimensional ground-state structure.

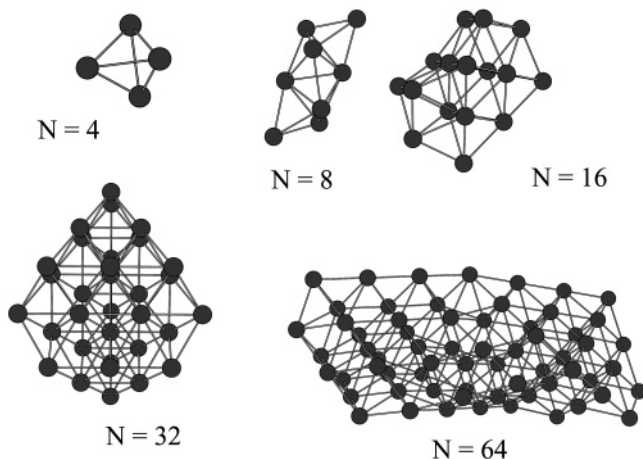


**Figure 6.** Ground-state clusters for  $N = 4, 8, 16, 32,$  and  $64$  for  $A = 0.05$  and  $\xi = 2.0$ .

size dependence of the gyration radius  $R_G$ , defined in terms of a particle's coordinates  $\mathbf{r}_i$  and center of mass coordinates  $\mathbf{R}_{CM}$  as

$$R_G = \frac{1}{N^{1/2}} \left[ \sum_{i=1}^N (\mathbf{r}_i - \mathbf{R}_{CM})^2 \right]^{1/2} \quad (3)$$

For spherical clusters,  $R_G \sim N^{1/3}$ ; for planar structures,  $R_G \sim N^{1/2}$ ; and for linear structures,  $R_G \sim N$ . Figure 7 shows that while in the pure short-range attractive case clusters retain their spherical shape for any size, in the case of addition of a repulsive potential only clusters of small enough size are spherical. On increasing  $N$ , the ground-state cluster structure becomes more and more linear. The sharp crossover size between spherical and linear cluster shape decreases on increasing  $A$  or  $\xi$ . Similarly, the linear cluster becomes thinner and thinner when repulsive effects become more and more relevant, as evidenced by the amplitude of the linear  $N$ -dependence of  $R_G$ . Once the linear cluster shape is established, the cluster energy increases linearly with the cluster size, resulting in the essentially flat  $N$ -dependence of the energy per particle (see Figure 4).

Three possible scenarios appear to take place in the cluster structure of the studied potential: (i) The first takes place for very small  $A$  values, where the repulsive energy is not sufficient to overcome the attractive contribution. Under these conditions, clusters are spherical and the standard behavior (infinite optimal size, liquid phase) is recovered. (ii) The second is an intermediate case, where a minimum in the cluster energy per particle is observed at an optimal size  $N^*$ , with a spherical cluster structure (for example, the case  $A = 0.2, \xi = 2$ ). Linear clusters can be built but with an energy slightly higher than that of the optimal cluster size. (iii) The third is a monotonically decreasing cluster energy per particle, ending in a flat curve, signaling equivalent stability for linear clusters of very different size (for example, the extreme case  $A = 7.93, \xi = 0.5$ ).

It is tempting to speculate that when parameters are chosen in such a way that linear growth is preferential,

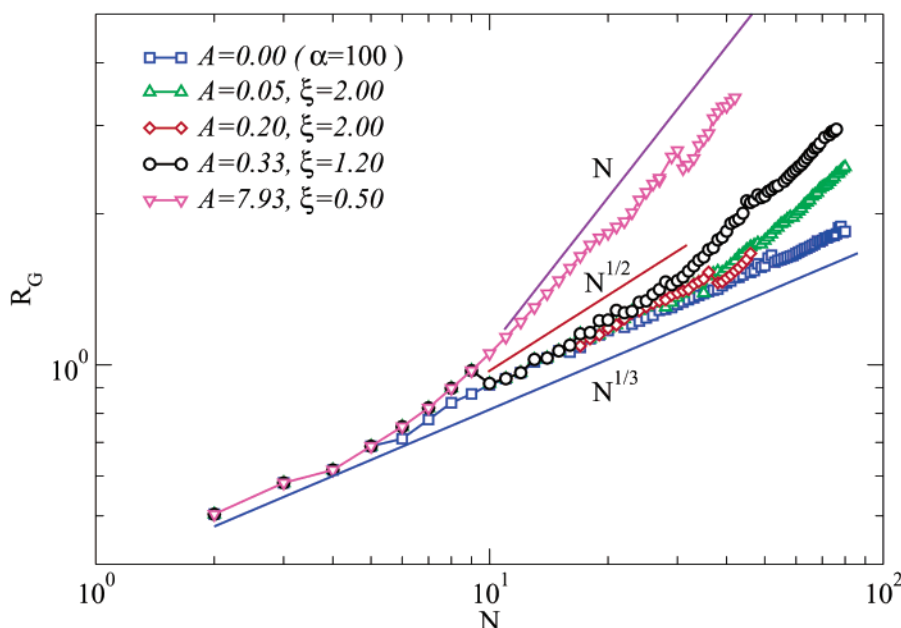


**Figure 7.** Size dependence of the gyration radius  $R_G(N)$  (in units of  $\sigma$ ) for all the considered potentials. The expected behaviors for spherical, planar, and unidimensional clusters, discussed in the text, are shown as solid lines.

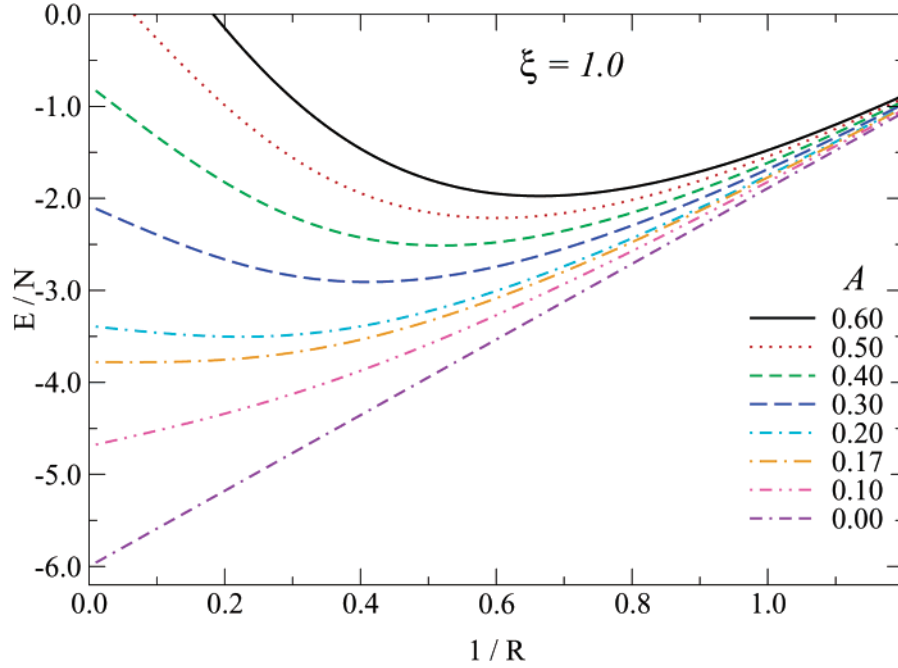


**Figure 8.** Energy per particle in the spherical approximation for  $\xi = 1.0$ , at the indicated values of  $A$ . A minimum starts to develop for values of  $A$  larger than a critical value  $A_c(\xi)$ .

at finite but small temperature (i.e., when structures different from the ground-state structure are also probed) clusters made of arms branching out from regions of locally higher energy can be generated. These structures, if macroscopic in size, would generate a gel-like structure, since no driving force for macroscopic aggregation is present (due to its inhibition caused by the repulsive term).

#### IV. The Spherical Case: The Crossover from Infinite to Finite Optimal Size

The numerical results presented in the previous sections confirm the possibility of creating stable clusters of optimal size, playing with the competition between the short-range attraction and the long-range repulsion. We have discussed the fact that in the limit of low temperatures and small packing fractions, that is, in the conditions where entropic contributions as well as cluster–cluster interactions can be neglected, the cluster ground-state energy  $E$  plays the role of relevant thermodynamic potential and, therefore, the minimum in  $E/N$  versus  $N$  provides an estimate of the stable cluster size  $N^*$ . Under these conditions, the system will partition into clusters of size  $N^*$  and no thermodynamic (macroscopic) coagulation will take place. Hence, the condition  $N^* = \infty$  acts as critical condition for the existence of a macroscopic phase separation as opposed to a phase made of clusters of finite size  $N^*$ .

To estimate the critical line separating the liquid phase ( $N^* = \infty$ ) from a cluster phase ( $N^*$  finite) in the  $(A, \xi)$  parameter space, it is necessary to calculate the ground-state energy for clusters of large size, which prevents the use of the “exact” numerical minimization which has been presented previously. An estimate of the critical line in the  $(A, \xi)$  space can be calculated analytically, under the hypothesis that clusters have a spherical shape and a homogeneous density of particles. The assumption of a spherical shape is expected to be valid in the region of parameter space where  $N^* = \infty$ , that is, where  $A$  or  $\xi$  is small and attraction is still dominant, as shown in the previous section. The numerical study of the  $N$ -dependence

of the ground state of the  $2\alpha - \alpha$  potential reported above shows that the  $N$ -dependence of the attractive part of the potential can be written as  $V_{2\alpha-\alpha}(N)/N = c_0 + c_1 N^{-1/3}$  with  $c_0 \approx -6$  and  $c_1 \approx 7.4$ . Since the value of the bulk energy ( $c_0$ ) reflects the energy of a very compact state (in which each particle is surrounded by 12 neighbors), the local density can be approximated with the local density of the fcc structure, providing a mean to convert the cluster radius  $R$  to the cluster size using  $N = \eta_{\text{fcc}}(2R/\sigma)^3$ , with  $\eta_{\text{fcc}} \approx 0.74$ .

To estimate the repulsive energy of a cluster of radius  $R \gg \sigma$ , we assume for simplicity a particle–particle radial distribution function  $g(r) = \Theta(r - \sigma)$  where  $\Theta$  is the Heaviside step function. This choice ensures that unphysical interactions, which would arise by pairs of points in the sphere closer than  $\sigma$ , are eliminated. A more precise calculation could be performed numerically by implementing a more detailed expression for  $g(r)$  (which, for example, could be calculated with the Verlet–Weiss  $g(r)$  for HS or with the known  $g(r)$  of the fcc structure). The simpler stepwise approximation used here is sufficient to predict the shape of the critical line. For large cluster sizes, the resulting expression for the cluster repulsive energy per particle is (see Appendix A)

$$\frac{E_Y(R)}{N} = \frac{3A\eta_{\text{fcc}}}{2\sigma^3} \xi^2 \left[ \frac{-24\xi^2(R + \xi)^2}{e^{2R/\xi} R^3} + \frac{16(\sigma + \xi)}{e^{\sigma/\xi}} - \frac{12(\sigma^2 + 2\sigma\xi + 2\xi^2)}{e^{\sigma/\xi} R} + \frac{\sigma^4 + 4\sigma^3\xi + 12\sigma^2\xi^2 + 24\sigma\xi^3 + 24\xi^4}{e^{\sigma/\xi} R^3} \right] \quad (4)$$

Figure 8 shows the  $1/R$  dependence of the cluster energy per particle, that is, the sum of the attractive and the repulsive part, for  $\xi = 1$  and several values of  $A$ . On increasing  $A$ , a progressive bending up of the curves takes place for large cluster radii, until for a critical value  $A_c$  ( $\approx 0.17$  for  $\xi = 1$ ), the slope of  $E(R)$  becomes flat at  $R =$

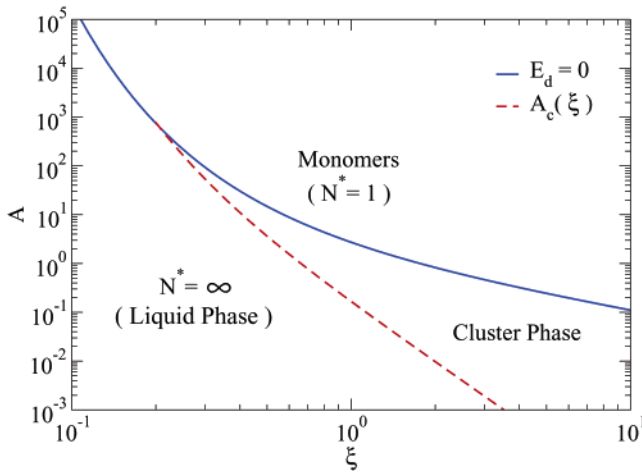


**Figure 9.** Critical line  $A_c(\xi)$  separating the  $N^* = \infty$  (liquid) from the cluster phase on the  $(A, \xi)$  parameter plane, together with the line of zero dimer energy  $E_d$ , separating clusters (either of finite or infinite size) from a phase of stable monomers.

$\infty$ , signaling that the lowest ground state does not require that all particles belong to the same cluster. For  $A > A_c$ , a minimum of  $E(R)$  arises at finite  $R$  value. To estimate the critical value of  $A(\xi)$ , the expression eq 4 for  $E_Y/N$  can be expanded in powers of  $1/R$ . At first order in  $1/R$ , we find

$$\frac{E_Y(R)}{N} \approx 24A\eta_{fcc}\frac{\xi^3}{\sigma^3}\left(\frac{\sigma}{\xi} + 1\right)e^{-\sigma/\xi} - 18A\eta_{fcc}\frac{\xi^4}{\sigma^3}\left(\frac{\sigma^2}{\xi^2} + 2\frac{\sigma}{\xi} + 2\right)e^{-\sigma/\xi}\frac{1}{R} \quad (5)$$

which provides, by adding the attractive part (also linear in  $1/R$ ) and setting the resulting coefficient of the  $1/R$  part to zero,  $A_c$  as a function of  $\xi$ ,

$$A_c(\xi) = \frac{c_1}{36\eta^{4/3}}\frac{\sigma^4}{\xi^4}\frac{\xi^2}{2\xi^2 + 2\xi\sigma + \sigma^2}e^{\sigma/\xi} \quad (6)$$

The critical line  $A_c(\xi)$ , shown in Figure 9 in the  $(A, \xi)$  plane, locates the region where, at low temperature, a phase of clusters of finite size is expected. For  $\xi \gg \sigma$ ,  $A_c \approx \xi^{-4}$ .

Finally, to provide an estimate of the region where even at  $T=0$  monomers are the stable state, we show in Figure 9 the line corresponding to the condition of the energy of a dimer  $E_d$  being zero; that is, along this line the pair potential repulsive energy at distance  $\sigma$  is equal to the short-range attractive energy (i.e.,  $Ae^{-\sigma/\xi}/(\sigma/\xi) = 1$ ). Crossing the  $E_d = 0$  line from below, the dimer ground-state energy goes from negative to positive values. The intersection of this line with the  $A_c(\xi)$  line suggests that for  $\xi \lesssim 0.2$ , there is no possibility of a cluster phase, with clusters larger than monomers. Therefore, for such small values of  $\xi$ , the ground state is given by an infinite cluster when the dimer energy is negative, crossing sharply to a solution of monomers when the dimer energy becomes slightly repulsive. Physical realization of cluster phases should then be searched in systems where the screening length is comparable to the particle size, that is, in weakly polar solvents or for small colloidal particles.

In concluding this section, it is worth recalling that, as seen in the previous section, for sizes comparable to or larger than  $N^*$ , the shape of the cluster becomes essentially linear and the spherical cluster calculations progressively

lose their meaning. Hence, the spherical calculations reported here should be limited to the case  $N^* = \infty$ , that is, below the critical  $A_c(\xi)$  line. Close to the critical line and above, more refined calculations accounting for almost linear cluster shapes should be performed.

## V. Conclusions

In this paper, we have studied, for a model where short-range attraction and long-range repulsion are simultaneously present, the structure and the energy of the ground state for clusters of different sizes. In these systems, microphase separated states, in the form of spherical (micellar) or columnar phases, arise spontaneously, due to the introduction of a new characteristic length provided by the balance between attractive and repulsive energies. Under the hypothesis of spherical clusters, an analytic evaluation of the cluster energy has been performed, providing a criterion for the existence of a cluster phase.

By varying the two parameters of the repulsive Yukawa potential, controlling respectively the amplitude of the repulsion and the screening length, clusters of different morphology, from almost spherical (for small  $A$  and  $\xi$  values) to almost one-dimensional (for larger  $A$  and  $\xi$  values), can be generated. The evaluation of the ground-state energy as a function of the cluster size gives evidence of a progressive tendency toward one-dimensional growth for all cases leading to cluster phases. This preferential one-dimensional growth is expected to enhance the stability of collective ordering into columnar or lamellar phases when cluster–cluster interactions are taken into account, both energetically and entropically,<sup>32</sup> in full agreement with the predictions for unscreened repulsive interactions.<sup>8–13</sup>

It is tempting to connect the one-dimensional growth followed by a dynamical arrest phenomenon, which is observed in several protein solution systems,<sup>33–36</sup> to the results discussed in the present article. Indeed, for these protein solutions, a change in temperature or in the solvent properties can trigger an aggregation process of proteins into cylindrical clusters. Under appropriate concentration conditions, these one-dimensional clusters further associate to form a macroscopic gel. The mechanisms discussed in this paper account for both the formation of cylindrical clusters and the insurgence of an effective vanishing surface tension, a condition necessary to stabilize a gel phase with respect to phase separation.<sup>37</sup>

Finally, we want to stress that in this study we have focused on isolated cluster properties and attempted to connect the cluster properties to the formation of a cluster phase, as opposed to a condensation of a dense liquid. In doing so, we have neglected the cluster–cluster interactions, which will play a very relevant role also at low temperatures, for packing fractions at which the cluster–cluster distance becomes comparable with the screening length. This will bring into play not only thermodynamic considerations but also, due to the low temperature, kinetic

(32) Onsager, L. *Phys. Rev.* **1942**, *62*, 558; *Ann. N.Y. Acad. Sci.* **1949**, *51*, 627.

(33) Le Bon, C.; Nicolai, T.; Durand, D. *Int. J. Food Sci. Technol.* **1999**, *34*, 451.

(34) Pouzot, M.; Nicolai, T.; Durand, D.; Benyahia, L. *Macromolecules* **2004**, *37*, 614.

(35) Renard, D.; Axelos, M. A. V.; Bouè, F.; Lefebvre, J. *Biopolymers* **1995**, *39*, 149.

(36) Manno, M.; San Biagio, P. L.; Palma, M. U. *Proteins: Struct., Funct., Bioinformatics* **2004**, *55*, 169 and references therein.

(37) Zaccarelli, E.; Sciortino, F.; Buldyrev, S. V.; Tartaglia, P. In *Unifying Concepts in Granular Media and Glasses*; Coniglio, A., Fierro, A., Herrmann, H. J., Nicodemi, M., Eds.; Elsevier B. V.: Amsterdam, 2004.

considerations. Preliminary work in this direction indeed suggests that slow-dynamics phenomena, related to the cluster–cluster repulsive interactions, may play a relevant role in arresting the equilibration of systems of particles interacting with the type of potential studied in this work.<sup>15</sup>

**Acknowledgment.** The authors acknowledge support from MIUR Cofin 2002, FIRB, and MRTN-CT-2003-504712. We thank A. Scala and J. Groenewold for helpful discussions.

### Appendix: Calculation of the Yukawa Cluster Energy

To evaluate the cluster energy, under the hypothesis of a homogeneous spherical cluster of number density  $\rho$ , we proceed in two steps: First we evaluate the potential energy of a particle located at distance  $x$  from the center of the sphere of radius  $R$ , by integrating all contributions from points located at the same distance  $r$  from the selected particle. Second, we evaluate the cluster energy by summing over all particles located at distance  $x$ , integrating  $x$  from 0 to  $R$ . The energy of a particle located at  $x$  inside a sphere of radius  $R$ ,  $W(R, x)$ , can be written as

$$W(R, x) = \rho \left[ 4\pi \int_0^{R-x} dr r^2 V_Y(r) g(r) + \int_{R-x}^{R+x} dr S(r; R, x) V_Y(r) g(r) \right] \quad (\text{A.1})$$

where  $S(r; R, x)$  is the surface generated by the intersection of two spheres of radius  $r$  and  $R$ , whose centers are located at distance  $x$  apart. From standard geometry,

$$S(r; R, x) = 2\pi r \left[ \frac{x^2 - r^2 + R^2}{2x} - (x - r) \right] \quad (\text{A.2})$$

The condition  $g(r) = \Theta(r - \sigma)$  acts in the integration limits providing two solutions, one for the case  $R - x < \sigma$  and one for the case  $R - x > \sigma$ ,

$$W(R, x) = \begin{cases} \rho \int_{\sigma}^{R+x} dr S(r; R, x) V_Y(r) & x > R - \sigma \\ \rho \left[ 4\pi \int_{\sigma}^{R-x} dr r^2 V_Y(r) + \int_{R-x}^{R+x} dr S(r; R, x) V_Y(r) \right] & x < R - \sigma \end{cases} \quad (\text{A.3})$$

The total potential energy of the cluster  $E_Y(R)$  is thus calculated as

$$E_Y(R) = 4\pi\rho \int_0^R dx W(R, x) \quad (\text{A.4})$$

For the case of the Yukawa potential, standard integration provides the result for  $E_Y(R)$  reported in eq 4. Indeed, after converting to energy per particle and using  $(\pi/6)\sigma^3\rho = \eta_{fcc}$ , one finds

$$\frac{E_Y(R)}{N} = \frac{3A\eta_{fcc}}{2\sigma^3} \xi^2 \left[ \frac{-24\xi^2(R + \xi)^2}{e^{2R/\xi} R^3} + \frac{16(\sigma + \xi)}{e^{\sigma/\xi}} - \frac{12(\sigma^2 + 2\sigma\xi + 2\xi^2)}{e^{\sigma/\xi} R} + \frac{\sigma^4 + 4\sigma^3\xi + 12\sigma^2\xi^2 + 24\sigma\xi^3 + 24\xi^4}{e^{\sigma/\xi} R^3} \right] \quad (\text{A.5})$$

LA048554T